Reliable determination of kinetics parameters of adatoms in thin-film epitaxy

X. D. Zhu*
Department of Physics, University of California at Davis, One Shields Avenue, Davis, California 95616-8677
(Received 11 May 1998; revised manuscript received 23 July 1998)

We show that in an interrupted step-flow epitaxy on a vicinal surface, the decay of adatom monomer density on terraces after deposition often has a simple dependence on the monomer diffusion coefficient D, the step-edge sticking probability S, and the extra step-edge energy barrier $E_{\rm step}$ (Schwoebel-Ehrlich barrier). One may reliably determine these kinetics parameters by examining the dependence of the *decay* rate constant on the average terrace width and the temperature. Such a decay can be monitored by either reflection high-energy electron diffraction or optical reflectance difference techniques. [S0163-1829(98)07840-0]

I. INTRODUCTION

Vapor-phase homoepitaxy and heteroepitaxy are two of the main growth techniques for fabricating new materials used in microelectronics, optoelectronics, and magnetic recording and storage media. These new materials are typically grown at high temperatures. This is necessary at high rates of deposition as newly arrived atoms need to have enough mobility to reach the edges of terraces to form flat films with atomically sharp interfaces. A number of kinetics parameters of adatoms determine the growth mode and in turn the quality of an epitaxially grown material.[1] They include the *surface diffusion coefficient* of adatom monomers, the *sticking probability* of an adatom arriving at the edge of a terrace, and the *extra energy barriers* for an adatom to descend the edge of a terrace. There are few techniques that can be used to measure these parameters at or close to the growth temperature around 700 K.

Neave and co-workers showed a method to indirectly deduce the adatom diffusion coefficient from the deposition rate at which the growth mode changes from a two-dimensional (2D) growth (through nucleation and growth and coalescence of monoatomically high islands) to a step-flow growth on a vicinal substrate.[2] It is based upon an assumption that in a continuous deposition and growth such a transition occurs when the diffusion length of a newly arrived adatom equals the terrace width before the next atom strikes the terrace. It is not, however, clear that the transition occurs *quantitatively* when this condition is reached. In fact, a reliable determination of surface diffusion coefficients requires a much more involved analysis of the transition from a 2D growth to a step-flow growth.[3,4]

Another technique involves scanning tunneling microscopic (STM) measurements of the saturation island density N_s as a function of the deposition flux at a given substrate temperature.[5] By invoking the nucleation theory,[6] one finds $N_s \sim \exp(-E_{\rm diff}/\gamma k_B T)$ where the factor γ is known once the critical island size is known. Unfortunately STM measurements of this type are carried out typically at below 160 K. Given the complexity of the morphology on a growth surface, it is not obvious that the kinetics parameters obtained at such low temperatures apply at 700–900 K where the step-flow growth occurs.

Another method is the optical diffraction technique developed by Zhu and co-workers and independently by Heinz and co-workers.[7,8] In this case, a periodic density distribution of adatoms or molecules is prepared on a substrate with the method of laser-induced desorption or atomic beam channeling through a laser standing wave, and the optical diffraction of a probe laser beam from such a distribution is subsequently monitored.[7–11] From the decay of the optical diffraction signal, one can extract the surface diffusion coefficient of adatoms. This technique is suited for measurements of surface diffusion of adatoms that are different from those of the substrate.[7,12,13] The implementation of such a method is still fairly involved at the present time, and it remains to be shown that it can yield diffusion kinetics parameters timely to meet the needs of material epitaxy.

It is desirable to explore other simpler and still direct experimental methods to measure kinetics parameters of adatoms under growth conditions. This is the subject of this paper. We find that by monitoring the decay of the adatom monomer density on terraces during an interrupted deposition and growth, one may reliably determine the adatom diffusion coefficient D, the sticking probability S at a step edge and the extra energy barrier for an adatom to descend a step edge (also known as Schwoebel-Ehrlich barrier). In an earlier paper, we have given a brief account of the key results of our investigation.[14] In the present paper, we describe the details of our theoretical consideration and the findings that were not reported earlier.

II. THEORETICAL CONSIDERATIONS

We consider an epitaxy consisting of sequences of interrupted deposition and growth in a step-flow growth regime rather than a continuous deposition and growth.[15,16] The epitaxy takes place on a crystalline surface vicinal to a low Miller index plane that exposes steps with an averaged width $L_{\rm terrace}$. $L_{\rm terrace}$ can be determined by a predetermined miscut angle. By limiting the consideration to a step-flow growth regime at high temperature, nucleation and growth *on* terraces can be neglected and we expect terraces to be covered mostly by adatom monomers. In addition, the interaction between monomers may also be neglected. By interrupting the deposition, we can follow the evolution of the monomer density as a result of growth at step edges. The temporal characteristics of the evolution are related to the kinetics parameters that we are interested in.

As a result of step-flow growth, the terraces are expected

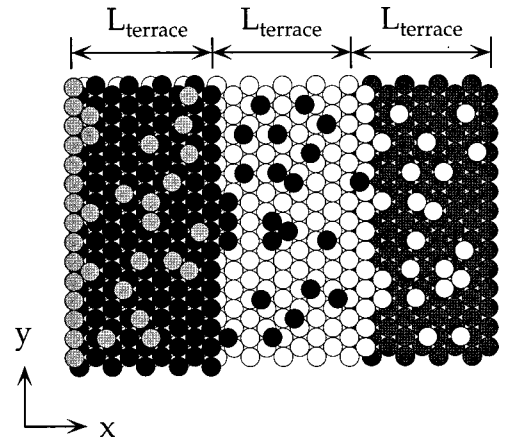

FIG. 1. A sketch of a vicinal substrate surface with a hexagonal lattice. During a step-flow epitaxy, the widths of terraces are roughly stabilized to a constant L_{terrace}. L_{terrace} is determined by a predetermined miscut angle.

to become roughly evenly spaced with an average width L_{terrace}. This is because that wider terraces receive proportionally more incident atoms and thus the corresponding upper step edges advance faster while narrower terraces receive proportionally less incident atoms and the corresponding upper step edges advance slower. During deposition, the monomer density increases at a rate proportional to the deposition flux. The equilibrium density of adatom monomers is determined by the balance between the deposition and the growth at step edges. The latter is usually *diffusion limited*. After the deposition is interrupted, the monomer density decreases as adatoms diffuse towards terrace edges and become attached. Assuming that there is no significant desorption, the total number of adatoms on the surface remains unchanged except that the number of adatom incorporated *within* terraces increases at the expense of monomers *on* terraces.

Since all step edges are expected to advance at roughly the same rate once the widths of terraces become stabilized, a terrace appears stationary with a fixed width L_{terrace} in a coordinate frame that rides with the advancing step edges. The evolution of the monomer density is governed by Fick's law in quasi-one-dimension that is perpendicular to step edges and the mass conservation. It is instructive to note that L_{terrace} establishes a length scale for mass transfer such that the evolution of the monomer density is expected to be described by structural factors $S(q,t)\sim\exp(Dq^2t)$ with wave vectors $q\sim 1/L_{\text{terrace}}$.[17,18] We show that this is indeed the case. Let the x axis be perpendicular to step edges and the y axis parallel to step edges. For illustration, we show in Fig. 1 a sketch of a model vicinal surface with adatoms on the terraces. Since both Fick's law and the mass conservation are satisfied locally, *we expect the monomer density to satisfy the diffusion equation in the coordinate frame that rides with the moving step edge*,[7,18]

$$\frac{\partial\theta}{\partial t}=D\,\frac{\partial^2\theta}{\partial x^2}. \tag{1}$$

θ is the adatom monomer coverage defined as the monomer number density divided by the density of the substrate surface atoms. The validity of Eq. (1) is further confirmed by our subsequent Monte Carlo simulation that will be described in the next section. Let $x=0$ be the edge adjoining the neighboring upper terrace, and $x=L_{\text{terrace}}$, the edge adjoining the neighboring lower terrace. In Fig. 2, we show a representative surface potential energy along a minimum energy path of diffusion for an adatom on and across a terrace. We take into account the possibility that an additional energy barrier E_{step} (i.e., Schwoebel-Ehrlich barrier[19]) may exist for an adatom to descend a step edge and another extra energy barrier E_a may also exist for an adatom to reach the step edge and settle down. The sticking probability of an adatom reaching the step edge at $x=0$ is thus given by $S=S_0\exp(-E_a/k_BT)$. The boundary condition at $x=L_{\text{terrace}}$ is determined by the requirement that the net flux is continuous.

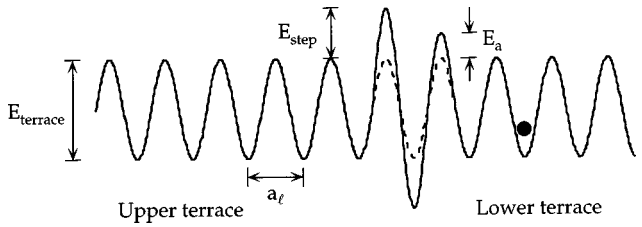

FIG. 2. A representative potential energy curve for an adatom (solid line) along a minimum energy path of diffusion on terraces and across a step edge. a_l is the separation between two neighboring energy minima. The dotted line indicates the potential energy curve on a terrace only.

$$-\frac{1}{\theta}\,\frac{\partial\theta}{\partial x}\bigg|_{x=L_{\text{terrace}}}=\left(\frac{\alpha_{\text{step}}}{a_l}\right). \tag{2a}$$

α_{step} is the probability of an adatom at $x=L_{\text{terrace}}$ to move forward by one lattice spacing a_l successfully. It has two contributions: one is the probability of a successful descent to the corner of the neighboring lower terrace and is given by $\exp(-E_{\text{step}}/k_BT)$;[1] the second is the probability of the corner site is being filled during a mean residence time τ_{res} as a result of diffusion and growth on the lower terrace and is given by $(a_l/4)(\partial\theta/\partial x)|_{x=0}$. The factor of $\frac{1}{4}$ comes from the fact that only one-quarter of the adatoms at one lattice spacing away from the step-edge corners will make the attempt to move towards these corners. Consequently, we have

$$\frac{1}{\theta}\,\frac{\partial\theta}{\partial x}\bigg|_{x=L_{\text{terrace}}}=-\left[\frac{\exp(-E_{\text{step}}/k_BT)}{a_l}+\frac{1}{4}\,\frac{\partial\theta}{\partial x}\bigg|_{x=0}\right]. \tag{2b}$$

Such a nonlinear boundary condition is the result of the fact that the edge of the lower terrace advances during growth and makes room for adatoms on the interrogated terrace. At low coverage as is case in the asymptotic limit of the growth after the deposition is interrupted, $|(\partial\theta/\partial x)|_{x=L_{\text{terrace}}}|\ll(\partial\theta/\partial x)|_{x=0}$ and thus Eq. (2b) is approximated by

$$\frac{1}{\theta}\,\frac{\partial\theta}{\partial x}\bigg|_{x=L_{\text{terrace}}}=-\,\frac{\exp(-E_{\text{step}}/k_BT)}{a_l}. \tag{2c}$$

The boundary condition at $x=0$ is also determined by the flux continuity:

$$\frac{1}{\theta}\frac{\partial\theta}{\partial x}\bigg|_{x=0}=\left(\frac{\alpha_0}{a_l}\right). \tag{3a}$$

Here α_0 is the probability of an adatom that is one lattice spacing away from the step-edge corner to become successfully attached subsequently. It also has two contributions: one is the probability that an adatom successfully makes a move towards the step-edge corner and is simple the sticking probability S; the second is the probability that a step-edge corner is being occupied as a result of descent of an adatom from the upper terrace such that the adatom at one lattice spacing away from the step-edge corner becomes automatically attached. The second part is given by $-(a_l/4)(\partial\theta/\partial x)|_{x=L_{\text{terrace}}}$. The negative sign takes into account the fact that $(\partial\theta/\partial x)|_{x=L_{\text{terrace}}}\leqslant 0$. Consequently, the boundary condition at $x=0$ is given by

$$\frac{1}{\theta}\frac{\partial\theta}{\partial x}\bigg|_{x=0}=\frac{S}{a_l}-\frac{1}{4}\frac{\partial\theta}{\partial x}\bigg|_{x=L_{\text{terrace}}}. \tag{3b}$$

In the asymptotic limit of the growth, we can ignore the second term on the right-hand side and Eq. (3b) is reduced to

$$\frac{1}{\theta}\frac{\partial\theta}{\partial x}\bigg|_{x=0}=\frac{S}{a_l}. \tag{3c}$$

It is noteworthy that if the sticking probability S is roughly unity, since $(\partial\theta/\partial x)|_{x=0}\sim\theta_{\max}/L_{\text{terrace}}$, we restore the well-known boundary at $x=0$ as $\theta(x=0)=\theta_{\max}(a_l/L_{\text{terrace}})\approx 0$.

We restrict our consideration to the low coverage limit $\theta\leqslant 0.3$ so that we can use Eq. (2c) and Eq. (3c) to solve for $\theta(x,t)$. The solution takes different forms depending upon the magnitudes of E_{step} and S.

(1) $a_l\exp(E_{\text{step}}/k_BT)\gg L_{\text{terrace}}$, but $a_l/S<L_{\text{terrace}}$.

In this case, the solution after the deposition is interrupted is given as follows:

$$\theta(x,t)=\sum_{n=1}\theta_{n0}\sin\left[\left(n-\frac{1}{2}\right)\pi\frac{x+a_l/S}{L_{\text{terrace}}+a_l/S}\right]\times\exp\left[-\left(n-\frac{1}{2}\right)^2\frac{\pi^2D}{(I_{\text{terrace}}+a_l/S)^2}t\right]. \tag{4}$$

θ_{n0}'s are determined from the initial condition right after the deposition. Most importantly, the asymptotic behavior of the monomer density is dominated by the first term,

$$\theta_1(x,t)\sim\theta_{10}\sin\left[\left(\frac{\pi}{2}\right)\frac{x+a_l/S}{L_{\text{terrace}}+a_l/S}\right]\times\exp\left[-\frac{\pi^2D}{4(L_{\text{terrace}}+a_l/S)^2}t\right]. \tag{5}$$

This means that the total number of monomers decays exponentially with an exponent $\beta_1\equiv\pi^2D/4(L_{\text{terrace}}+a_l/S)^2$. As we have expected qualitatively, the exponent is proportional to the adatom diffusion coefficient D on terraces and the proportionality constant $\pi^2/4(L_{\text{terrace}}+a_l/S)^2$ is inversely proportional to the square of an effective terrace width $L_{\text{terrace}}+a_l/S$.[1] By following the total number or the coverage of adatoms monomers with, for example, optical reflectance difference or reflection high-energy electron diffraction (RHEED) from the vicinal surface, one can extract the decay exponent β_1. From the dependence of β_1 on the mean terrace width L_{terrace} and temperature, one can in turn determine a number of important kinetics parameters of adatoms during step-flow epitaxy. For example, one can measure a set of decay exponents β_1 at various temperatures and with different mean terrace widths L_{terrace}. L_{terrace} can be changed by miscutting substrates at different angles. Care has to be taken to ensure that there is no substantial step bunching within the ranges of temperatures and miscut angles. One can then plot the inverse of the square root of β_1 versus L_{terrace},

$$\frac{1}{\sqrt{\beta_1}}=\frac{2}{\pi}\frac{L_{\text{terrace}}+a_l/S}{\sqrt{D}}. \tag{6}$$

The slope of $1/\sqrt{\beta_1}$ gives $(2/\pi\sqrt{D})$ and in turn the monomer diffusion coefficient D. From the intercept $(2/\pi\sqrt{D})(a_l/S)$, one extracts the sticking probability S. Furthermore from the temperature dependence of D, one can determine both the diffusivity D_0 and the activation energy barrier E_{terrace} on terraces.

(2) $a_l/S\gg L_{\text{terrace}}$ and $a\ \exp(E_{\text{step}}/k_BT)<L_{\text{terrace}}$.

The solution takes a slightly different form,

$$\theta(x,t)=\sum_{n=1}\theta_{n0}\cos\left[\left(n-\frac{1}{2}\right)\pi\frac{x}{L_{\text{eff}}}\right]\times\exp\left[-\left(n-\frac{1}{2}\right)^2\frac{\pi^2D}{L_{\text{eff}}^2}t\right], \tag{7}$$

with an effective terrace width given by $L_{\text{eff}}=L_{\text{terrace}}+a_l\exp(E_{\text{step}}/k_BT)$. In the asymptotic limit, the adatom monomer density is dominated by

$$\theta_1(x,t)\sim\theta_{10}\exp\left[-\frac{\pi^2D}{4[L_{\text{terrace}}+a\ \exp(E_{\text{step}}/k_BT)]^2}t\right]. \tag{8}$$

From the dependence of the exponent $\beta_2\equiv\pi^2D/4[L_{\text{terrace}}+a_l\exp(E_{\text{step}}/k_BT)]^2$ on L_{terrace} and temperature, we can again obtain the adatom diffusion coefficient D and now the extra step edge barrier E_{step}. By plotting the inverse of the square root of β_2 versus L_{terrace},

$$\frac{1}{\sqrt{\beta_2}}=\frac{2}{\pi}\frac{L_{\text{terrace}}+a_l\exp(E_{\text{step}}/k_BT)}{\sqrt{D}}, \tag{9}$$

the slope yields the diffusion coefficient D, and the intercept yields a $\exp(E_{\text{step}}/k_BT)$. By measuring the temperature dependence of the intercept and the slope, one can determine both E_{terrace} and E_{step}.

(3) $a_l\exp(E_{\text{step}}/k_BT)<L_{\text{terrace}}$ and $a_l/S<L_{\text{terrace}}$.

The solution is given by the following expression:

$$\theta(x,t)=\sum_{n=1}\theta_{n0}\sin\left[n\pi\frac{x+a_l/S}{L_{\text{eff}}}\right]\exp\left[-\frac{n^2\pi^2D}{L_{\text{eff}}^2}t\right]. \tag{10}$$

The effective terrace width is given by $L_{\text{eff}}=L_{\text{terrace}}+a_l/S+a_l\exp(E_{\text{step}}/k_BT)$. The asymptotic limit of the monomer density is dominated by

$$\theta_1(x,t) \sim \theta_{10} \times \exp\left[- \frac{\pi^2 D}{[L_{\text{terrace}} + a_l/S + a_l \exp(E_{\text{step}}/k_B T)]^2} t \right]. \quad (11)$$

The decay exponent $\beta_3 \equiv \pi^2 D/[L_{\text{terrace}} + a_l/S + a_l \exp(E_{\text{step}}/k_B T)]^2$ can be determined experimentally and used to extract the diffusion coefficient. Again by plotting the inverse of the square root of β_3 versus L_{terrace},

$$\frac{1}{\sqrt{\beta_3}} = \frac{L_{\text{terrace}} + a_l/S + a_l \exp(E_{\text{step}}/k_B T)}{\pi \sqrt{D}}, \quad (12)$$

we find the diffusion coefficient D from the slope and $a_l/S + a_l \exp(E_{\text{step}}/k_B T)$ from the intercept. Generally, one cannot separate the contributions to the intercept from the sticking probability S and the finite Schwoebel-Ehrlich barrier. If one knows *a priori* that $S \sim 1$, the intercept may be used to determine E_{step}. If on the other hand E_{step} is known *a priori* to be small such that $a_l \exp(E_{\text{step}}/k_B T) \sim a_l$, the intercept may be used to extract S.

It is noteworthy that if the decay exponent β varies with L_{terrace} at all, a_l/S and $a_l \exp(E_{\text{step}}/k_B T)$ cannot be both much larger than L_{terrace}. In this case, by fitting the decay of the monomer density to a single exponential function with an exponent β, one obtains a good estimate of the diffusion coefficient $D \sim 4L_{\text{terrace}}^2 \beta/\pi^2$ from just one value of L_{terrace} without any *prior* knowledge of S and E_{step}.

Before leaving this section, we briefly consider the situation where the terrace widths on a vicinal surface vary over a range about the mean L_{terrace}. This situation is realistic as one always has a distribution of terrace widths on a real vicinal surface. Clearly if the distribution is too wide such that there is really not a characteristic length scale for terrace widths, we do not expect the decay of the monomer density to have simple dependence on L_{terrace}. In this case we cannot use the present analysis to determine kinetics parameters. If the distribution is a few tens of a percent or less about the mean L_{terrace}, we show here that it is still feasible to use the present analysis to extract kinetics parameters reliably.

To make the analysis more tractable, we assume that the terrace width has a Gaussian distribution centered at L_{terrace} with a standard deviation of δ. In the asymptotic limit, it is easily shown that after averaging Eq. (8) for example over the distribution of terrace widths, we arrive at

$$\langle \theta_1(t) \rangle \approx \frac{1}{\sqrt{1 + \pi^2 D \delta^2 t/(L_{\text{terrace}} + a_l/S)^2}} \times \exp\left[- \frac{\pi^2 D t}{4(L_{\text{terrace}} + a_l/S)^2 + 4\pi^2 D \delta^2 t} \right]. \quad (13)$$

If $\delta = 0.25 L_{\text{terrace}}$, the correction to Eq. (8) becomes noticeable only after a time $t \sim 8(L_{\text{terrace}} + a_l/S)^2/\pi^2 D$ when the exponential factor or $\langle \theta_1(t) \rangle$ has dropped by a factor over 100. Before this time Eq. (8) is a very good approximation. As we will show in the following Monte Carlo simulation study, $t \sim 8(L_{\text{terrace}} + a_l/S)^2/\pi^2 D$ is long enough to observe the asymptotic behavior of the monomer density. If the standard deviation of the terrace width distribution is more than 50% of the mean L_{terrace} we will not be able to use the above analysis to extract S and E_{step} reliably. However, as long as there is noticeable dependence of the decay rate on the mean terrace width L_{terrace}, $D \sim 4L_{\text{terrace}}^2 \beta/\pi^2$ is still a very good estimate.

III. MONTE CARLO SIMULATION

We now address three issues through a Monte Carlo simulation of an interrupted step-flow growth on a vicinal surface: (1) the validity of Eq. (1); (2) the upper limit of the monomer density below which the analysis described in the previous section applies; (3) the asymptotic limit beyond which the adatom monomer density decays exponentially.

We have performed a Monte Carlo simulation of a noninteracting lattice gas on a square lattice with $400a_l$ along the x axis and $2000a_l$ along the y axis as sketched in Fig. 1. To simulate a vicinal surface, we make the first column of the lattice the initial upper terrace edge, the next 200 columns the terrace under interrogation so that the terrace width L_{terrace} is $200a_l$, and the remaining 199 columns the lower terrace. Initially, we randomly deposit adatoms on the terrace of interest to a coverage of $\theta = 0.5$. We subsequently allow adatoms to execute random walk. Considering a noninteracting lattice gas is reasonable in the step-flow growth regime as the substrate temperature is generally high so that 2D island formation is expected to be unstable and adatoms behave *approximately* as an assemble of noninteracting monomers.[1,6] For the purpose of addressing the above three issues, it is sufficient to perform simulations for the case where (1) E_{step} is large and thus adatoms cannot descend to the lower terrace and adatoms cannot ascend to the upper terrace either; (2) the sticking coefficient S is unity; (3) the diffusion of adatoms along a step edge is fast so that an atom at the step edge always finds and settles down at a site with the maximum possible bond coordination. To take the effect of step flow into consideration in the mean field sense, once an adatom becomes attached and settles down at a stable corner site at the edge of the terrace, we also fill the corner site on the neighboring lower terrace that is $L_{\text{terrace}} = 200a_l$ away from this site so that the lower terrace corner site becomes the new edge of the interrogated terrace. This procedure computationally leads to the even flow of the step edges. If Eq. (1) is valid, we expect the Monte Carlo simulation to yield results predicted by Eqs. (4) and (5). This is indeed the case.

We record the monomer coverage profile after each time interval of $\Delta t = 0.2\tau_{\text{res}} \times (L_{\text{terrace}}/a_l)^2 = 8000\tau_{\text{res}}$. τ_{res} is the residence time of an adatom at an isolated site on a terrace. The tracer diffusion rate of such an atom is given by $D = a_l^2/4\tau_{\text{res}}$. As shown in Ref. 14, even just after one time interval $\Delta t = 8000\tau_{\text{res}}$ where the adatom monomer coverage is still as high as 0.34, the distribution of the adatom coverage is already well described by two sinusoidal functions as predicted by Eq. (4),

$$\theta(x,t) \sim \theta_1 \sin\left(\frac{\pi}{2L_{\text{terrace}}} x \right) + \theta_3 \sin\left(\frac{3\pi}{2L_{\text{terrace}}} x \right). \quad (14)$$

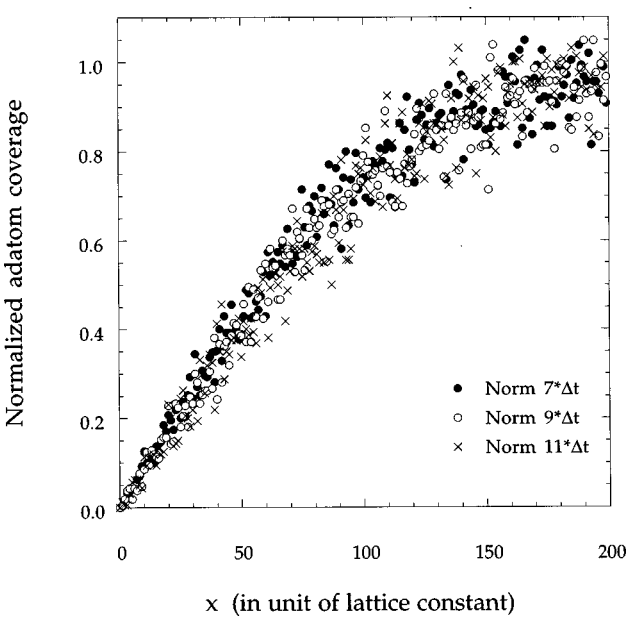

FIG. 3. Adatom coverage profiles normalized to the mean value near $x=L_{\text{terrace}}$ after $t=7^*\Delta t$ ($\Delta t=8000\tau_{\text{residence}}$). The profiles fit very well to $\sin(\pi x/2L_{\text{terrace}})$.

After $7\Delta t=56\,000\tau_{\text{res}}$ when the adatom coverage drops to 0.12, the profile is well described by Eq. (5) or

$$\theta(x,t)\sim\theta_1(t)\sin\left(\frac{\pi}{2L_{\text{terrace}}}x\right). \tag{15}$$

In fact the adatom density profile after $7\Delta t=56\,000\tau_{\text{res}}$ no longer changes except for the overall magnitude as shown in Fig. 3. The profiles in Fig. 3 fit $\sin(\pi x/2L_{\text{terrace}})$ essentially perfectly. Also as shown in Ref. 14, the spatially averaged adatom coverage was fit well to a double exponential function. We found that the slow (asymptotic) decay component varies with time $t=N\Delta t$ as $\exp(-\alpha_1 N)=\exp(-0.124N)$. The exponent 0.124 agrees within 1% with the theoretical value of $\pi^2 D\Delta t/4L^2_{\text{terrace}}=0.2(\pi/4)^2=0.1234$ from Eq. (5). The fast decay component has an exponent α_2 three time as large as α_1, as expected from Eqs. (4) or (14). The excellent agreement between the Monte Carlo simulation and our analytical analysis shows that in the frame that moves with advancing step edges Eq. (1) is indeed valid for describing the evolution of the adatom monomer density under step-flow growth condition. It also shows that even at coverages as high as $\theta=0.34$, it is sufficient to use Eq. (2c) and Eq. (3c) for boundary conditions. Furthermore, the asymptotic limit is already reached when $\exp(-\beta t)=\exp(-\pi^2 Dt/4L^2_{\text{terrace}})<0.3\sim0.4$. This means that as soon as the monomer density drops by 40–30 % from the value immediately after the deposition is interrupted, Eq. (5) can be used to extract kinetics parameters as discussed in the previous section.

IV. EXPERIMENTAL DETERMINATION OF THE ASYMPTOTIC DECAY OF THE MONOMER DENSITY ON TERRACES OF A VICINAL SURFACE

The evolution of the adatom monomer density can be monitored with either electron reflection such as low-energy electron diffraction (LEED) and RHEED (Refs. 15, 16, and 20) or optical reflection including normal-incidence[21] and oblique-incidence linear reflectance difference spectroscopy,[16] surface photoabsorption spectroscopy,[22] ellipsometry,[23,24] reflected optical second-harmonic generation,[25,26] and reflected sum-frequency generation.[27] Linear optical reflection techniques are more commonly used than nonlinear optical techniques as the absolute signal strengths are much larger and the implementation is simpler. RHEED is much more commonly used than LEED to monitor the growth mode and quality of a thin-film epitaxy.

In the case of RHEED, one monitors *coherent* specular reflection and higher-order diffractions of collimated high-energy electrons (10–20 keV) from a vicinal surface. At a low coverage θ of adatom monomers, the random positions of these adatom monomers relative to each other cause the electron reflection from these adatoms to be out of phase. As a result these monomers do not contribute to the *coherent* specular reflection and higher-order diffractions of electrons. The intensities of the specular RHEED and higher-order RHEED deviate from their corresponding maxima by

$$I_{n,\max}-I_n(\theta)\approx 2I_{n,\max}\theta. \tag{16}$$

By monitoring the asymptotic recovery of either the specularly reflected RHEED $I_0(\theta)$ or the first-order RHEED $I_1(\theta)$ in an interrupted deposition and growth, one should be able to measure the kinetics parameters as described in the previous section. To the best of our knowledge, RHEED has not been used for this purpose despite its extensive use in monitoring epitaxy.

Optical reflectance difference spectroscopies and ellipsometry are alternative methods for monitoring the adatom monomer density on terraces.[16,22–24] Since optical wavelengths are much larger than a lattice constant a_l, it may seem unusual that optical reflection at such a long wavelength should be sensitive at all to the rearrangement of adatoms on the scale of lattice constant. Such rearrangements include the growth at step edges at the expense of monomers *on* terraces. The sensitivity of optical reflection to atomic rearrangement on a surface derives from the change in optical dielectric response in the outermost surface layer. During the recovery of an interrupted deposition and growth sequence, the optical polarizability of an adatom monomer is being replaced by that of an adatom that is incorporated in a terrace. The reflectance difference is proportional to the difference of optical polarizabilities before and after the *incorporation* and the monomer density. Zhu and co-workers recently used an oblique-incidence optical reflectance difference technique to monitor interrupted deposition and growth of $SrTiO_3$ on $SrTiO_3(001)$.[16] They showed that the reflectance difference signal $S(\theta)$ is given by[16,28]

$$S(\theta)\sim\left[\text{Re}\left(\frac{r_p-r_{p0}}{r_{p0}}\right)-\text{Re}\left(\frac{r_s-r_{s0}}{r_{s0}}\right)\right]\sim\theta \tag{17}$$

and therefore it varies linearly with the adatom coverage θ. Here r_p and r_s are the reflectivities of the surface for p and s polarization, respectively, in the presence of adatom monomers on terraces, while r_{p0} and r_{s0} are the reflectivities in the absence of adatom monomers. From the temperature dependence of the decay exponent of $S(\theta)$, these authors were able to deduce the surface diffusion energy barrier of $SrTiO_3$ or a mobile component of it on terraces of $SrTiO_3(001)$. In

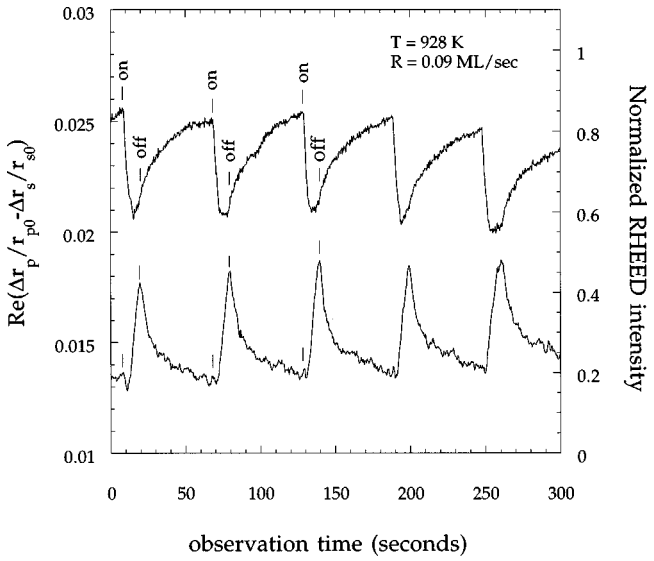

FIG. 4. Simultaneously measured oblique-incidence optical reflectance difference and specular RHEED intensity from a vicinal $SrTiO_3(001)$ during five cycles of interrupted deposition and step-flow growth of $SrTiO_3$. The asymptotic behaviors of both signals are described well by single exponential functions.

Fig. 4, we reproduce the results of optical reflectance difference and specular RHEED intensity measurements of interrupted deposition and growth sequences of $SrTiO_3$ on a vicinal $SrTiO_3(001)$.[16] The recovery of the optical signal and RHEED intensity are well described with single exponential functions.

V. CONCLUSION

We have shown a simple and reliable method to measure kinetics parameters of adatoms or molecular adsorbates under the epitaxial step-flow growth condition. Such a method is easily implemented in most vapor-phase epitaxy systems.

As to the limitations of our present analysis, we have assumed that there is negligible 2D nucleation and most adatoms on terraces are in the form of monomers. In cases when there is a substantial nucleation, one needs to invoke the appropriate nucleation theory to separate the effect of nucleation and dissociation of 2D islands from the effect of monomer diffusion on the recovery of the optical reflectance difference or RHEED signals. We have also assumed that the diffusion rate along a step edge is fast compared to the growth rate so that step edges remain straight and parallel to each other. This analysis fails if the growth at the step edges is of dendritic form due to the lack of adatom mobility along step edges. In this case, the average width of the terraces is *ill defined* and the recovery of the optical or RHEED monitoring signals is no longer related to the adatom surface diffusion kinetics in a simple way.

ACKNOWLEDGMENTS

This work was supported in part by the National Science Foundation under Grant No. DMR-94-03441. Acknowledgment is also made to the donors of Petroleum Research Fund, administered by the ACS, for partial support of this research.

*Electronic address: xdzhu@physics.ucdavis.edu

[1] J. Tersoff, A. W. Denier, and R. M. Tromp, Phys. Rev. Lett. **72**, 266 (1994).
[2] J. H. Neave *et al.*, Appl. Phys. Lett. **47**, 100 (1985).
[3] Y. Kajikawa *et al.*, Surf. Sci. **265**, 241 (1992).
[4] T. Nishinaga and K. Cho, Jpn. J. Appl. Phys., Part 1 **27**, L12 (1988).
[5] Y.-W. Mo *et al.*, Phys. Rev. Lett. **66**, 1998 (1991); R. M. Tromp *et al.*, *ibid.* **55**, 1303 (1985); H. Brune *et al.*, *ibid.* **73**, 1955 (1994); M. Bott *et al.*, *ibid.* **76**, 1304 (1996).
[6] J. A. Venables, Philos. Mag. **27**, 697 (1973).
[7] X. D. Zhu *et al.*, Phys. Rev. Lett. **61**, 2883 (1988); Xudong Xiao *et al.*, *ibid.* **66**, 2352 (1991); X. D. Zhu, Mod. Phys. Lett. B **6**, 1217 (1992).
[8] G. A. Reider *et al.*, Phys. Rev. Lett. **66**, 1994 (1991).
[9] P. A. Williams, G. A. Reider, Leping Li, U. Höfer, T. Suzuki, and T. F. Heinz, Phys. Rev. Lett. **79**, 3459 (1997).
[10] G. L. Timp *et al.*, Phys. Rev. Lett. **69**, 1636 (1992); J. J. McClelland *et al.*, Science **262**, 877 (1993); R. W. McGowan *et al.*, Opt. Lett. **20**, 2535 (1995).
[11] X. D. Zhu, Opt. Lett. **24**, 1890 (1997).
[12] X. D. Zhu, A. Lee, A. Wong, and U. Linke, Phys. Rev. Lett. **68**, 1862 (1992).
[13] G. X. Cao, E. Nabighian, and X. D. Zhu, Phys. Rev. Lett. **79**, 3696 (1997).
[14] X. D. Zhu, Phys. Rev. B **57**, R9478 (1998).
[15] M. Y. Chern *et al.*, J. Vac. Sci. Technol. A **11**, 637 (1993).
[16] X. D. Zhu *et al.*, Phys. Rev. B **57**, 2514 (1998).
[17] D. Forester, *Hydrodynamic Fluctuations, Broken Symmetry, and Correlation Functions* (Benjamin, London, 1975), p. 10.
[18] R. Gomer, Rep. Prog. Phys. **53**, 917 (1990).
[19] R. L. Schwoebel and E. J. Shipsey, J. Appl. Phys. **37**, 3682 (1966); G. Ehrlich and F. G. Hudda, J. Chem. Phys. **44**, 1030 (1966).
[20] H. Koinuma and M. Yoshimoto, Appl. Surf. Sci. **75**, 308 (1994).
[21] D. E. Aspnes *et al.*, Phys. Rev. Lett. **59**, 1687 (1987); D. E. Aspnes *et al.*, J. Vac. Sci. Technol. A **6**, 1327 (1987); D. E. Aspnes *et al.*, *ibid.* **9**, 870 (1991); J. P. Harbison *et al.*, Appl. Phys. Lett. **52**, 2046 (1988); D. E. Aspnes *et al.*, *ibid.* **52**, 957 (1988).
[22] N. Kobayashi and Y. Horikoshi, Jpn. J. Appl. Phys., Part 2 **28**, L1880 (1989); **29**, L702 (1990); K. Nishi *et al.*, Appl. Phys. Lett. **61**, 31 (1992).
[23] B. Drevillon, Prog. Cryst. Growth Charact. **27**, 1 (1993).
[24] K. Hingerl *et al.*, Appl. Phys. Lett. **63**, 885 (1993).
[25] H. W. K. Tom, C. M. Mate, X. D. Zhu, J. E. Crowell, T. F. Heinz, G. A. Somorjai, and Y. R. Shen, Phys. Rev. Lett. **52**, 348 (1984).
[26] T. F. Heinz *et al.*, in *Advances in Laser Science III* (American Institute of Physics, New York, 1988), p. 452.
[27] X. D. Zhu, H. Suhr, and Y. R. Shen, Phys. Rev. B **35**, 3047 (1987); J. H. Hunt, P. Guyot-Sionnest, and Y. R. Shen, Chem. Phys. Lett. **133**, 189 (1987).
[28] A. Wong and X. D. Zhu, Appl. Phys. A: Mater. Sci. Process. **63**, 1 (1997).